JMEPEG (2002) 11:265-273

Heat Transfer at the Metal/Substrate Interface During Solidification of Pb-Sn Solder Alloys

K. Narayan Prabhu, S.T. Kumar, and N. Venkataraman

(Submitted 26 August 2001)

Heat transfer analysis during the solidification of lead, tin, and two lead-base solder alloys against two different chill materials (steel and copper) was carried out with and without flux coating on the chill surface. Temperatures at two known locations inside the chill and casting were recorded as the casting started solidifying, and the acquired chill temperature data were used for solving a one-dimensional heat conduction equation inversely to yield the metal/chill interfacial heat flux and chill surface temperature as a function of time. The initial heat flux was high due to good contact at the metal/chill interface. As the casting started solidifying, there was a reduction in the heat flux due to the nonconforming contact at the interface. Chills with flux coating resulted in finer microstructures near the solder/substrate interface compared to those obtained with uncoated chills. The fineness of the microstructure also increased when copper was used as the chill material. The estimated total heat flow was found to be higher with flux-coated and copper chills. This was in good agreement with the finer microstructures obtained near the solder/chill interfacial region for solidification against copper chills and chills with flux coating on their surface.

Keywords Pb-Sn solder alloys, solder/substrate, solidification

1. Introduction

Soldering is the oxide-free bonding of similar or dissimilar metals by a filler metal that has a lower melting point than the metals to be joined and is carried out at temperatures ≤400 °C. The wetting of the solder alloy to the base metal is the key requirement to achieve bonding, and the process involves neither diffusion nor the melting of the base metal.

In soldering, a sound joint is obtained only when the surfaces are absolutely clean and contain no oxide films. However, in actual practice the surfaces of the substrate materials are tarnished and contain oxide layers. To enable wetting to take place, generally a flux with sufficient reactivity is employed at the soldering temperature to remove oxide films from the surface of the work piece and to favor the easy bonding of the solder alloy to the substrate material. The flux material can be organic or inorganic. The mechanism of bond formation and the action of fluxes during the soldering process have been discussed in great detail by Manko.[1]

The difficulties inherent in the solidification of most metals are present in the case of solder solidification as well. For example, many solder alloys exhibit shrinkage upon solidification and cooling, and this leads to the formation of an air gap between the solidifying metal and the base metal surface.[2] The presence of any air gap at the mold/metal interface during casting solidification would result in a decrease in the thermal contact conductance, reducing the heat transfer both across the interface and in the solidifying metal. In soldering, this will strongly reduce the strength of the joint by limiting the contact between the solder and the base metal. The formation of an air gap or a nonconforming contact at the interface during soldering depends upon the ability of the molten solder alloy to flow over and wet the base metal. This can be influenced by several parameters, such as the surface roughness of the base metal, solder composition, type of flux used, and the temperature of the liquid solder.[1-3]

The use of solidification simulation techniques has made possible the prediction of temperature distribution and shrinkage defects in sand and die-castings of pure metals and alloys.[4] The methodology also can be extended to the solidification of solder alloys. However, the success of a numerical simulation technique depends on a reliable database on the thermophysical properties of the solder alloy and, more significantly, on the heat transfer coefficient (h) specified at the solder/base metal interface.[5]

Depending on the material properties and the solidifying metal, the following three types of interfaces may exist:

K. Narayan Prabhu, S.T. Kumar, and **N. Venkataraman,** Department of Metallurgical and Materials Engineering, Karnataka Regional Engineering College, Surathkal, P.O. Srinivasnagar 574 157, Karnataka, India. Contact e-mail: prabhu@chaithra.krec.ernet.in.

Nomenclature

C_p	specific heat (J/kg K)
k	thermal conductivity (W/m K)
h	thermal contact conductance (W/m^2 K)
q	interfacial heat flux (W/m^2)
R	future temperatures-1
t	time (s)
T	estimated temperatures (°C)
Y	Measured temperatures (°C)
Δt	time step for temperature (s)
$\Delta\theta$	time step for heat flux (s)
ϕ	sensitivity coefficient
ρ	density (kg/m^3)

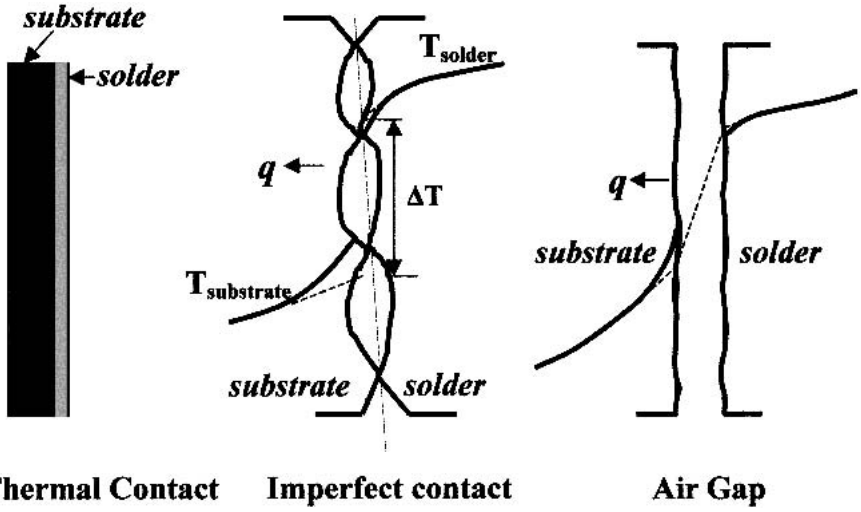

Fig. 1 A schematic representation of the solder/substrate interface

- Perfect thermal contact between the substrate and the solidifying skin;
- Imperfect contact between the substrate and the solidifying skin; and
- A gap of finite thickness separating the metallic surface and the solidifying skin.

These conditions are shown schematically in Fig. 1.[5] In the first case, heat transfer takes place only by conduction. In the second case, the overall heat transfer coefficient may be written as the sum of the three components.[6]

$$h = h_s + h_c + h_r$$

where

h_s = the part due to solid conduction through the points of contact;
h_c = the heat transfer coefficient due to gas conduction; and
h_r = the radiation heat transfer coefficient.

The third type of interface shows the formation of an air gap, resulting in the lowering of heat flux. The air gap offers a resistance to the heat transfer from the solidifying casting to the base metal and is the most important phenomenon controlling the solidification of the alloy on metallic chills.[7] The overall heat transfer coefficient 'h' in this case may be given as:

$$h = h_c + h_r$$

where, h_c is the heat transfer coefficient resulting from gas conduction across the gap and h_r is the heat transfer coefficient resulting from radiation.

Convective heat transfer can usually be neglected for the typical range of interfacial gap widths. The heat transfer resulting from radiation is insignificant due to the low temperatures involved during solder solidification.

The first type of thermal contact is the most desirable in all metal-joining processes, including soldering. But an ideal thermal contact is not expected to exist at the solder/substrate interface in actual practice. In real situations, the solder metal may contact the base metal through a large number of microscopic contact points, as shown in the second type of interface. The third type of interface representing the formation of an air gap is the least desirable and indicates no bonding, with a clear separation between the base metal and the solder alloy.

The overall heat transfer coefficient at the solder/base metal interface is called thermal contact conductance, which is calculated as:

$$h = \frac{q}{\Delta T}$$

where q is the solder/base metal interfacial heat flux, and ΔT is the temperature drop across the solder/base metal interface. The interface plays a major role during the solidification of the alloy in high-conductivity moulds.[8-10] A good thermal contact conductance at the interface would therefore result in better quality for the solder joint.

Hence, it is essential to assess the heat transfer at the solder/base metal interface. This can be achieved by carrying out inverse modeling, which involves the numerical estimation of solder/substrate interfacial heat flux from the measured thermal history inside the substrate and the solder.[11,12]

Generally, the soldering process involves the solidification of a small quantity of the alloy against a metallic substrate. The total heat content of the solidifying metal is very low. The use of thermocouples may disturb the temperature field in the interfacial region, and this may introduce errors into the estimation of the heat flux. Hence, in the present work, the thermal contact heat transfer at the metal/substrate interface was assessed during the solidification of cylindrical castings of lead, tin, and two Pb-Sn solder alloys, with copper and steel as the substrate materials. The aim was to study the effect of the substrate material and the flux coating on the heat transfer at the solder/substrate interface. An attempt has been made to correlate the interfacial heat transfer to

the fineness of the metallurgical microstructure of the solder metal near the solder/metal interface.

2. Experimental

A schematic sketch of the experimental set-up for the measurement of interfacial heat flux transients, during the upward solidification of Pb-Sn alloys against a metallic chill, is shown in Fig. 2. Pure lead, tin, 63Sn-37Pb, and 80Pb-20Sn solder alloys were selected as the casting materials. The set-up consisted of a cylindrical sand mould that was prepared using a CO_2 process with a circular chill located at the bottom. Circular chills of copper and steel with a 25 mm diameter and a 40 mm height were used. The thermophysical properties of the chill materials are given in Table 1.

The chill located at the bottom of the mould was instrumented with two 1 mm K-type mineral-insulated thermocouples. The thermocouples were located exactly at the nodal points. The thermal history at these locations was used for the estimation of heat transfer during casting solidification. The solidifying casting was instrumented with K-type thermocouples enclosed in twin-bore alumina beads. All the thermocouples were connected by means of coaxial cables to a portable data logger that was interfaced with a computer.

The pure metal/alloy was melted in an electrical resistance-type furnace. The molten metal was poured into the CO_2 sand mould with chill at the bottom. Experiments were carried with and without flux coating on the chill material. A flux material consisting of a eutectic mixture of zinc chloride and ammonium chloride in the ratio of 3:1 was used in the present investigation. This composition has been found to be very effective for soldering because of its lower melting point of 176 °C, compared to the higher melting point of the solder alloys.

Specimens for metallographic examination were prepared using casting sections taken from a point 10 mm from the chill/metal interface. The surface preparation was carried out initially on a belt grinder. The specimens were subsequently polished on different grades of emery paper. The final surface preparation was carried out on a polishing disc to obtain a scratch-free mirror finish. Levigated alumina was used as the polishing abrasive. The polished specimen was washed and dried. The specimen surface was then etched for nearly 7 min using an etchant having the following composition: 3 parts glacial acetic acid, 4 parts concentrated nitric acid, and 16 parts water. The temperature was maintained at around 42 °C during the etching.

3. Estimation of Heat Flux

A mathematical model was developed to estimate the interfacial heat flux from the measured temperatures inside the chill during the solidification of the solder alloy.

The one-dimensional heat conduction equation,

$$\frac{\partial^2 T}{\partial x^2} = \frac{\rho C_p}{k}\left(\frac{\partial T}{\partial t}\right) \quad \text{(Eq 1)}$$

was solved inversely using the method of Beck.[13,14] ρ, C_p, and k are the density, specific heat, and thermal conductivity of the chill material, respectively. In this inverse technique, the surface heat flux density is estimated from the temperatures measured inside a heat-conducting solid. This was done by minimizing, at regular finite difference time intervals, the function

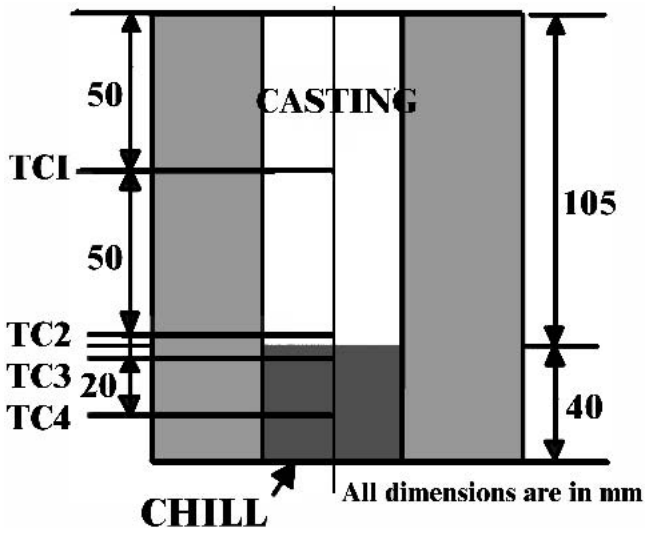

Fig. 2 A schematic sketch of the casting/chill set-up

Table 1 Thermophysical Properties of the Chill Materials

Material	Thermal Conductivity (W/mK)	Density (kg/m^3)	Specific Heat (J/kgK)
Copper	363	8960	423
Steel	42	7860	418

$$F(q) = \sum_{i=1}^{MR} (T_n - Y_n)^2 \quad \text{(Eq 2)}$$

where $M = \Delta\theta/\Delta t$ and R = a small integer. T_n and Y_n are calculated and measured temperatures, respectively, at a location close to the surface of the solid. $\Delta\theta$ and Δt are the time steps for the estimation of heat flux and temperature, respectively. In the present work, the temperatures recorded by thermocouple TC3 were taken as Y_n. The temperatures recorded by TC4 were used as the known boundary condition in the estimation of the unknown boundary heat flux.

The unknown boundary condition q (0,t) and the temperature Y (t) were vectorized, with $\Delta\theta$ as 1 s and Δt as 0.5 s. Assuming that $q$lm is known ($q_m^0 = 1$ initially), q_m^{l+1} was estimated as follows. The superscript l and the subscript m denote the iteration number and the time step for the heat flux, respectively. The function F (q) was minimized by an iterative procedure using the Taylor series expansion.

$$T_n^l \approx T_n^{l-1} + \frac{\partial T_n^{l-1}}{\partial q_m^l}(q_m^l - q_m^{l-1}) \quad \text{(Eq 3)}$$

The partial derivative in the above equation is called the sensitivity coefficient, which is denoted by ϕ, and was calculated using

$$\phi_i^{l-1} = \frac{T_n\,(q_m^{l-1}\,(1+\xi)) - T_n(q_m^{l-1})}{\xi q_m^{l-1}} \qquad \text{(Eq 4)}$$

where ξ is a small number, taken as 0.001 in the present calculations.

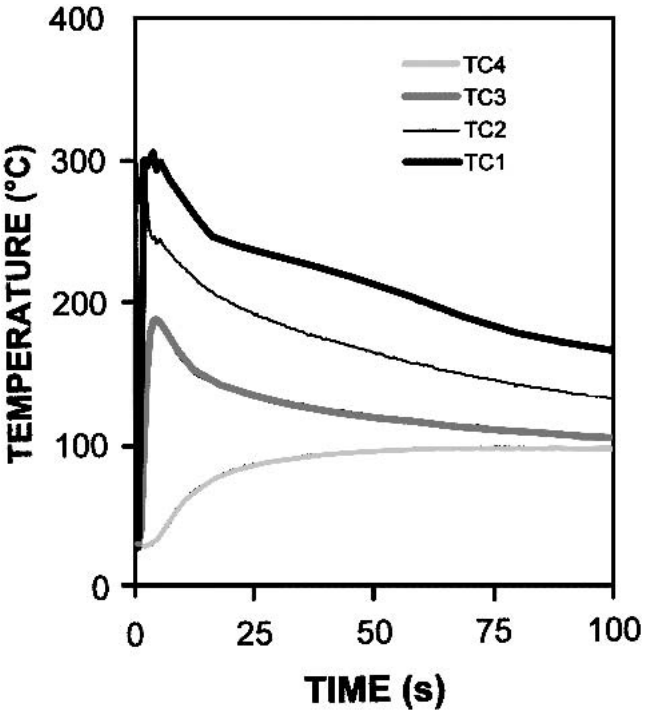

Fig. 3 A typical casting and chill thermal history during the solidification of a solder alloy

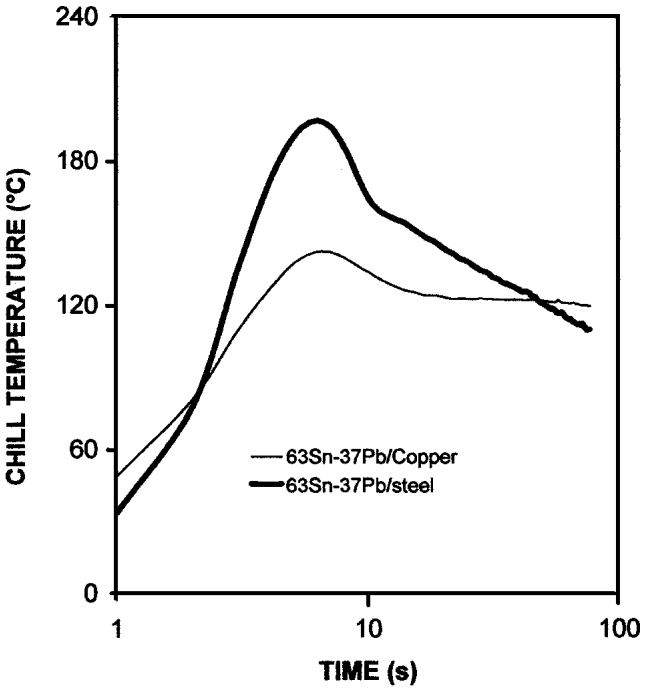

Fig. 4 Effect of chill material on chill surface temperature

Applying the condition $\partial F/\partial q = 0$ on Eq (2) for minimization, introducing Eq 3 into Eq 2, and differentiating with respect to q_m^l, the correction in q at each iteration step was as follows:

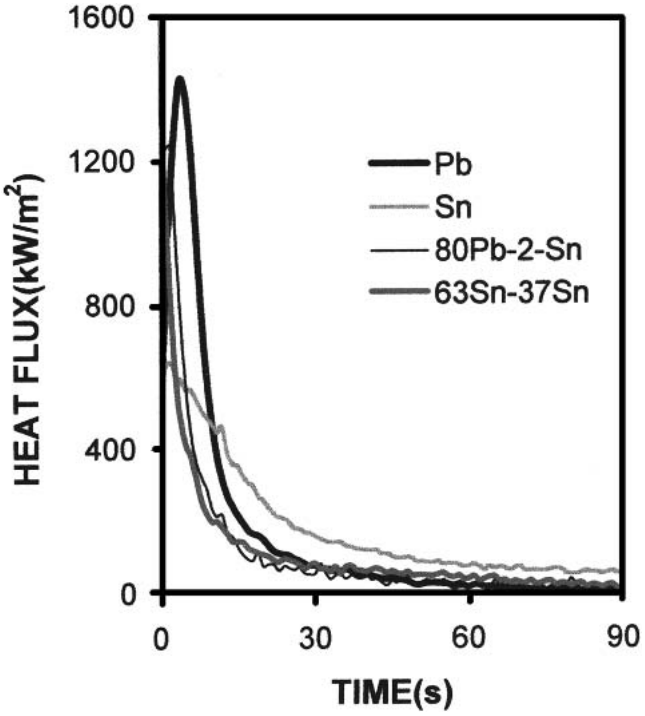

Fig. 5 Heat flux transients during solidification against an uncoated steel chill

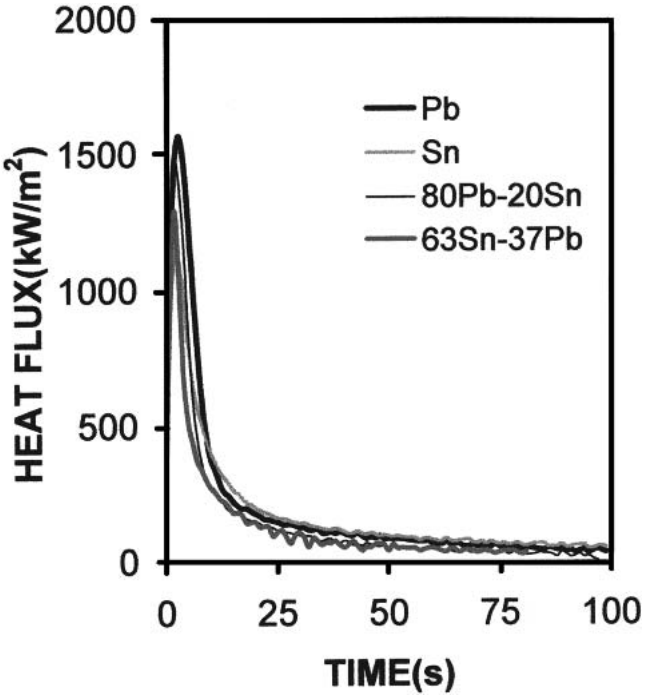

Fig. 6 Heat flux transients during solidification against a steel chill with flux coating

$$\nabla q_m^{l-1} = \frac{\sum_{i=1}^{MR} (Y_n - T_n^{l-1})\phi_i^{l-1}}{\sum_{i=1}^{MR} (\phi_i^{l-1})^2} \quad \text{(Eq 5)}$$

where

$$\nabla q_m^l = q_m^l - q_m^{l-1}$$

The correction for heat flux (∇q) at each iteration step was estimated, and the procedure continued until the ratio ($\nabla q/q$) was less than a predetermined limit. The final iterated value of q^m was used as the initial heat flux q_{m+1}^0 for the next time step m + 1. The inverse modeling technique adopted yielded the sand surface temperature (T_m) and the interfacial heat flux (q).

4. Results and Discussion

Figure 3 shows a typical casting and chill thermal history during the solidification of pure lead vertically upward against the copper chill incorporated in a sand mould. The temperatures recorded by the casting thermocouples showed a maximum temperature after a time interval of about 3 s for all the experiments. The gap of 3 s taken by the thermocouples to record the peak temperature was due to the time taken for the filling of the casting and the response time of the thermocouples. This was followed by a continuous fall in temperature up to the melting point of the alloy. The fluctuation in the cooling curves above the melting point could be due to the turbulence in the molten metal.

The chill thermal history that is shown in Fig. 3 indicates that the locations near the interface heated rapidly to a maximum temperature. After the occurrence of peak, the chill temperature decreased at a slower rate compared to the initial rate of heating. At the location away from the interface, the temperature gradually increased and remained constant.

Steel chills were heated to maximum temperature compared to copper chills (Fig. 4). This was due to the lower thermal diffusivity of steel chills (α for steel $= 12.4 \times 10^{-6}$ m^2/s; α for copper $= 114.1 \times 10^{-6}$ m^2/s at 273 K), which resulted in a slower conduction of heat from the surface of the steel chill to the outer surface.

The use of a flux coating on the chill surface resulted in better wetting compared to a bare surface. For example, the surfaces of castings of 63Sn-37Pb that were solidified against chills coated with flux were welded to the chill surfaces and could not be easily separated. The application of flux removes oxide films on the chill surface and improves the wetting characteristics of the liquid metal that is in contact with the chill material. This is in contrast to die-castings in which the insulating coating on the die surface reduces the heat flow from the casting to the die-wall and prevents the welding of the liquid metal onto the die surface. The application of flux resulted in higher heating rates for the chill material. For example, the peak heating rates at 2 mm from the interface for the copper chill with and without flux coating were found to be 67.5 °C/s and 45 °C/s, respectively, during the solidification of the 63Sn-37Pb alloy.

The estimated heat flux transients at the interface are shown in Fig. 5-8. As the liquid metal fills the cavity of the mould, super heat is dissipated from the liquid metal to the chill. This is shown in the casting surface temperature curve as a rapid

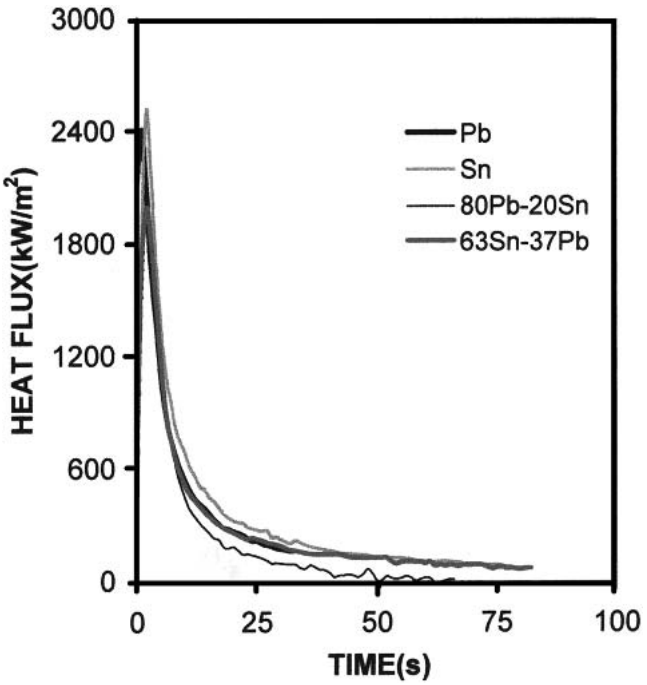

Fig. 7 Heat flux transients during solidification against an uncoated copper chill

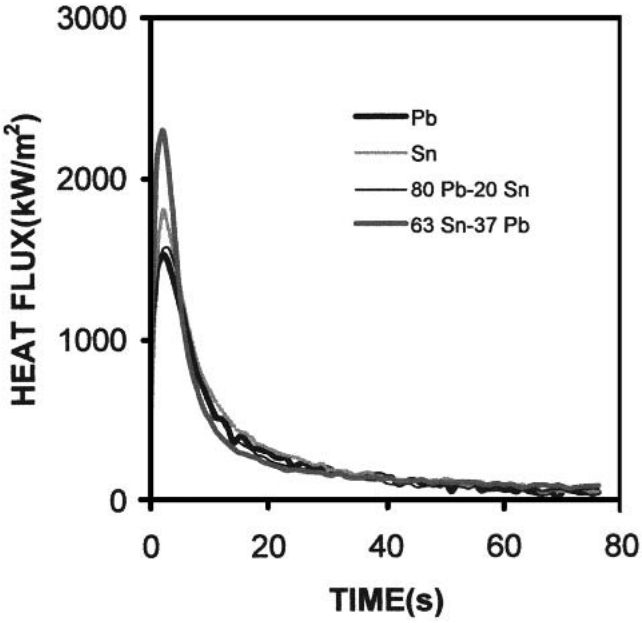

Fig. 8 Heat flux transients during solidification against a copper chill with flux coating

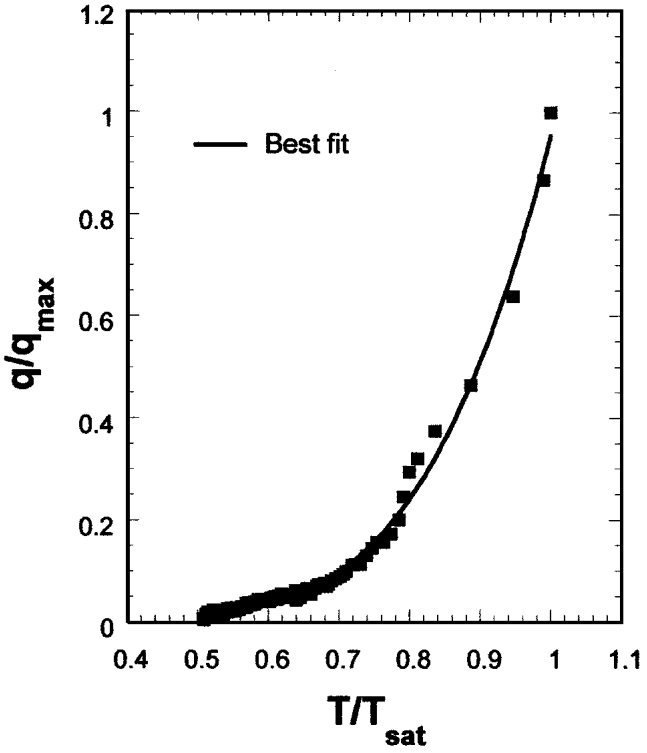

Fig. 9 Variation of normalized flux with normalized chill surface temperature for 63Sn-37Pb solder alloy and uncoated steel chills

decrease in the casting temperature. Below the liquidus temperature, a solid skin is formed. Since the skin is weak, it may be pushed against the chill surface by metallostatic pressure of the liquid metal. This may result in intimate contact between chill surface and the casting skin. Since good contact is made between the chill surface and the casting skin, the heat flux rapidly rises to a maximum. At the same time, the casting skin temperature drastically drops. This drop in casting surface temperature results in a thickening of the casting shell. As the thickness of the solidified shell increases, the strength increases, which can resist the metallostatic pressure. This results in a contraction of the casting skin away from the chill surface, causing the formation of an air gap. The time would be associated with the transformation of the interfacial condition from a perfect contact to a nonconforming contact. The time of occurrence of peak heat flux was nearly 5 s after the start of pouring. Heat flux transients were significantly higher for copper chills compared to steel chills. The heat flux transients increased significantly with the application of flux coating on the chill surfaces. For example, the peak heat flux during the solidification of the 63Sn-37Pb alloy against copper chill with and without flux coating was found to be 2305 kW/m^2 and 1995 kW/m^2, respectively. This could be attributed to an improved metal/chill interfacial contact condition that was a result of the removal of surface oxide films on the application of flux coating.

To model the heat flux as a function of chill temperature, plots of normalized heat flux temperatures (q/q_{max}) versus normalized chill surface temperatures (T/T_{sat}) were constructed for pure lead and two solder alloys solidifying under various conditions. Typical variations of normalized flux with normalized

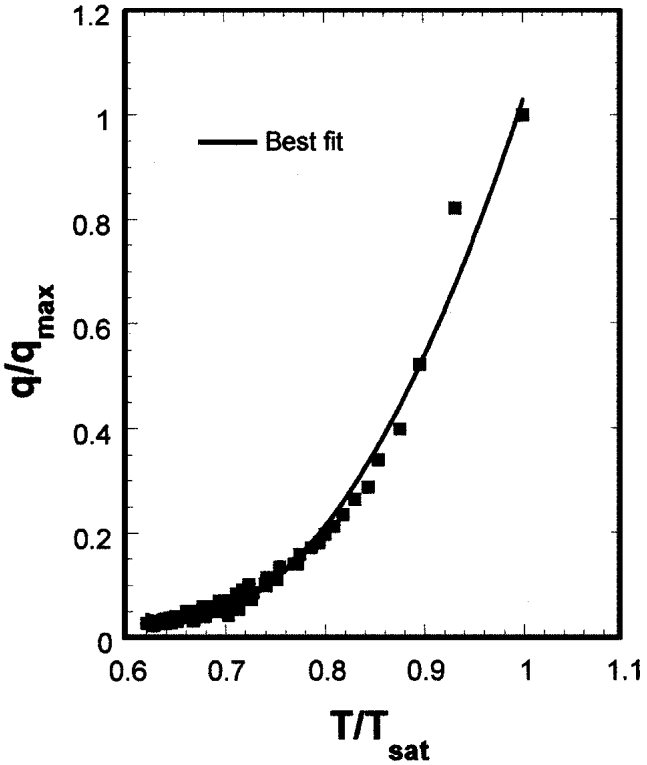

Fig. 10 Variation of normalized flux with normalized chill surface temperature for the 63Sn-37Pb solder alloy and flux-coated steel chills

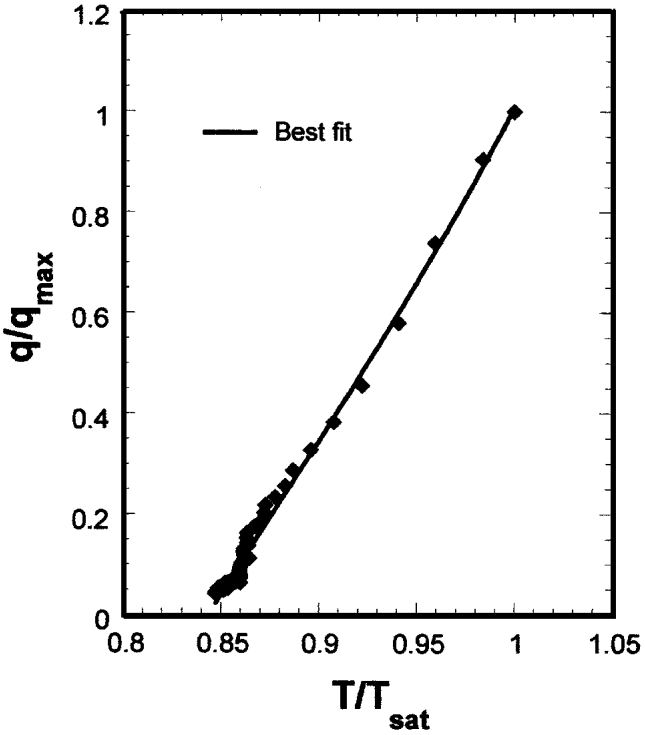

Fig. 11 Variation of normalized flux with normalized chill surface temperature for the 63Sn-37Pb solder alloy and uncoated copper chills

chill surface temperature are shown in Fig. 9-12. The peak surface temperature of the chill material was taken as the chill saturation temperature, T_{sat}. The peak flux and chill saturation temperatures were assumed to occur at the same time, although a maximum variation of 4 s was observed. This variation was neglected while estimating the normalized flux and chill temperature parameters.

The variation of q/q_{max} with T/T_{sat} could be represented by a polynomial equation of the type

$$\frac{q}{q_{max}} = A + B\left(\frac{T}{T_{sat}}\right) + C\left(\frac{T}{T_{sat}}\right)^2 + D\left(\frac{T}{T_{sat}}\right)^3 \quad \text{(Eq 6)}$$

where A, B, C, and D are regression constants.

It was observed that a small drop in the chill surface temperature from T_{sat} resulted in a large decrease in the heat transfer rates. This decrease in the heat flux increased significantly when copper was used as the chill material. For example, a 10% decrease in the chill surface temperature resulted in a 49% decrease in the heat transfer rate for the 63Sn-37Pb alloy solidifying against steel. The corresponding decrease for copper was found to be 66%. The effect of coating was marginal in the case of steel chills and was found to be significant for high-conductivity copper chills.

Figures 13 and 14 show the integral heat flux curves computed for two solder alloys solidifying against steel and copper chills, respectively. The curves indicate the total heat extracted by the chills at any instant of time. Higher values of heat flow were obtained with coated chills. For example, for the 63Sn-37Pb alloy the total heat flow at a time of 10 s was 12,900 kJ/m^2 for a flux-coated copper chill compared to 11,000 kJ/m^2 for an uncoated copper chill. The corresponding values for coated and uncoated steel chills were found to be 6300 and 5300 kJ/m^2, respectively.

Figures 15-18 show photomicrographs of lead/tin alloys solidifying against steel/copper chills. It was observed that the structure became finer for copper chills compared to steel chill. This is because of the higher heat extracted from the casting by

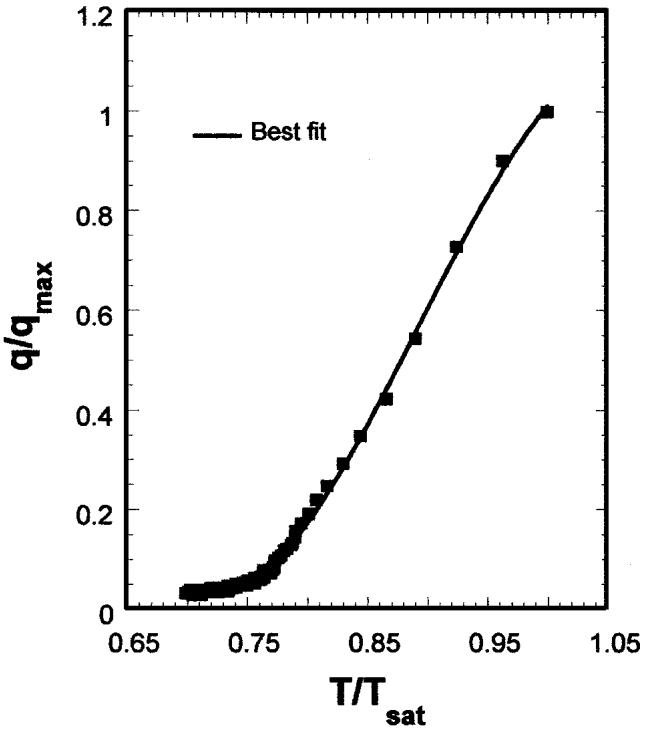

Fig. 12 Variation of normalized flux with normalized chill surface temperature for the 63Sn-37Pb solder alloy and flux-coated copper chills

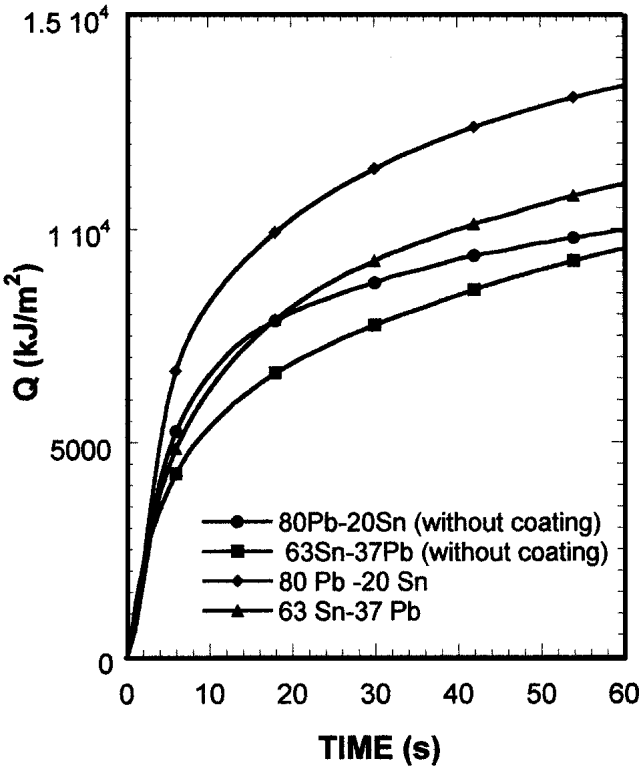

Fig. 13 Integral heat flow curves for the solidification of two solder alloys against flux-coated and uncoated steel chills

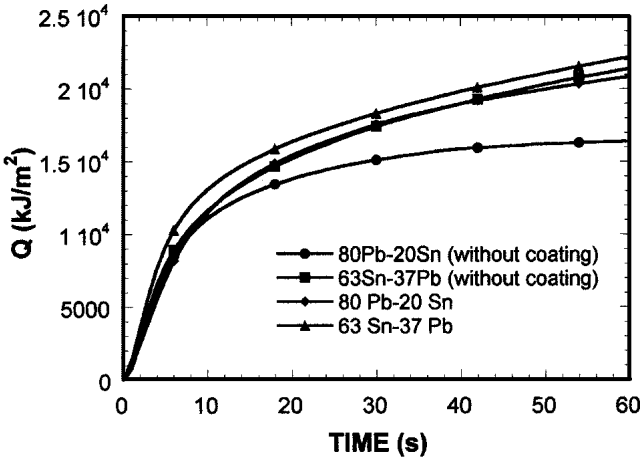

Fig. 14 Integral heat flow curves for the solidification of two solder alloys against flux-coated and uncoated copper chills

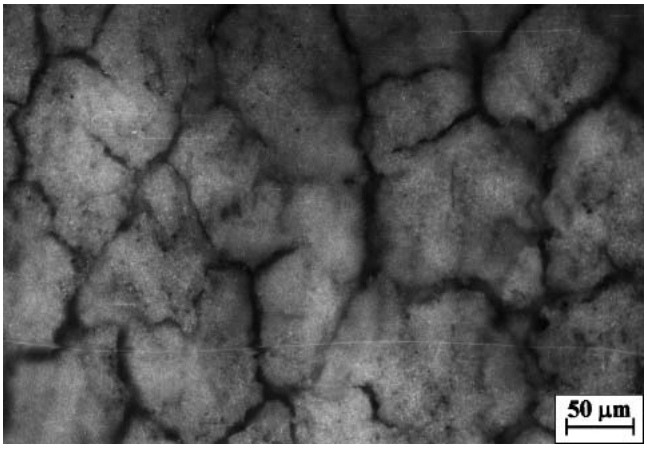

Fig. 15 Photomicrograph of the casting at 5 mm from the chill/metal interface for the 63Sn-37Pb solder alloy and uncoated steel chill

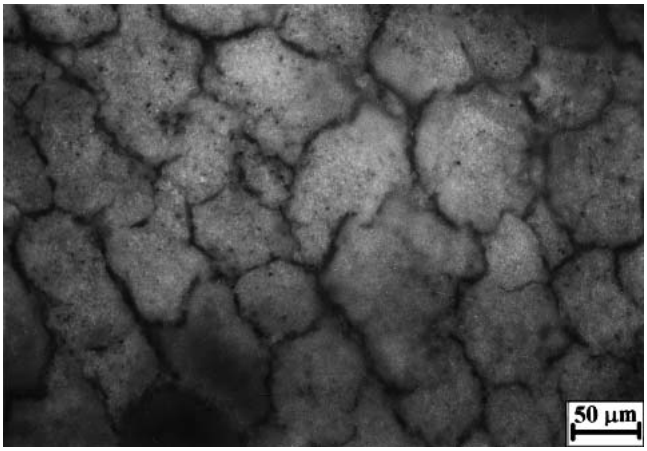

Fig. 16 Photomicrograph of the casting at 5 mm from the chill/metal interface for the 63Sn-37Pb solder alloy and flux-coated steel chill

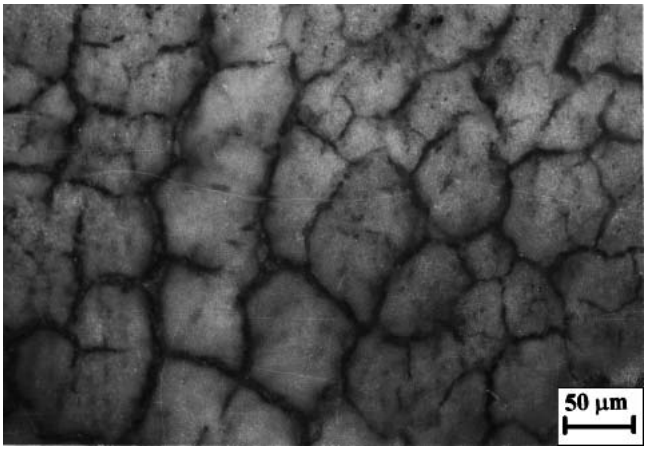

Fig. 17 Photomicrograph of the casting at 5 mm from the chill/metal interface for the 63Sn-37Pb solder alloy and uncoated copper chill

the copper chill. Furthermore, it was observed that a flux coating on the chill surface resulted in higher heat extraction, resulting in a finer structure. For example, the average grain sizes at 5 mm from the solder/substrate interface for the 63Sn-37Pb

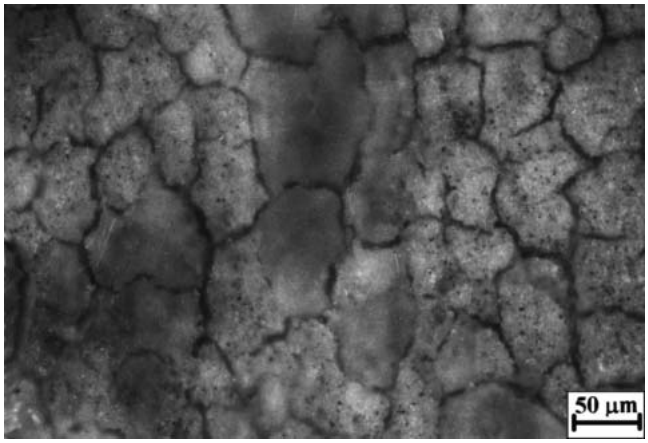

Fig. 18 Photomicrograph of the casting at 5 mm from the chill/metal interface for the 63Sn-37Pb solder alloy and flux-coated copper chill

eutectic alloy against flux-coated copper, copper, flux-coated steel, and steel chills were found to be 44, 53, 58, and 80 μm, respectively.

5. Conclusions

Based on the results and discussion, the following conclusions were drawn.

- The thermal contact heat transfer during the solidification of two lead-base solder alloys against metallic substrates was assessed using an inverse analysis, and the resulting interfacial heat flux transients are reported. The heat flux curves indicated a maximum after pouring for all the solder/metal combinations. The peak heat flux could be associated with a good solder/substrate contact condition existing at the interface.
- Copper chills resulted in higher heat flux transients (q_{max} for 63Sn-37Pb alloy = 1995 kW/m^2) compared to steel chills (q_{max} = 1289 kW/m^2) for all the experiments. The application of flux coating on the surface of the metal substrate increased the rates of heat transfer.
- The normalized heat flux transients were modeled as functions of normalized chill surface temperatures.
- Integral heat flux curves were computed for the solder alloys investigated, and the curves indicated higher heat flows for solidification against flux-coated chills.
- The flux-coated chills resulted in a finer grain structure in the contact region of the solidified solder alloy. The higher thermal conductivity of the copper chill also improved the fineness of the microstructure. The integral heat flow parameters indicated a good correlation with the fineness of the microstructure in the region of the solder/substrate interface.

References

1. H.H. Manko: *Solders and Soldering,* McGraw-Hill Co., New York, NY, 1964, pp. 1-25.
2. D.R. Durham: "Numerical Simulation of Solder Solidification," *Welding Res.*, 1979, Oct.(suppl), pp. 301-05.
3. W.D. Griffiths: "A Model of the Interfacial Heat Transfer Coefficient during Unidirectional Solidification of an Aluminium Alloy," *Met. Mat. Trans. B*, 1999, *30B*, pp. 473-82.

4. T. Veerabadran, S.K. Manna, and H.L. Gegel: "Simulation Based Process Design of Castings: It Pays Off," *IIF Trans.*, 1995, pp. 116-23.
5. T.S. Prasanna Kumar and K.N. Prabhu: "Heat Flux Transients at the Casting/Chill Interface During Solidification of Aluminium Base Alloys," *Met. Trans. B*, 1991, *22B*, pp. 717-22.
6. K. Ho and R.D. Pehlke: "Mechanisms of Heat Transfer at a Metal/Mold Interface," *AFS Trans.*, 1984, *92*, pp. 587-97.
7. K. Narayan Prabhu and John Campbell: "Investigation of Casting/Chill Interfacial Heat Transfer during Solidification of Al-11% Si Alloy by Inverse Modelling and Real-Time X-ray Imaging," *Int. J. Cast Metals Res.*, 1999, *12*, pp. 137-43.
8. L.J.D. Sully: "The Thermal Interface Between Castings and Chill Moulds," *AFS Trans.*, 1976, *84*, pp. 735-44.
9. E.S. Tillman and J.T. Berry: "Influence of Thermal Contact Resistance on the Solidification Rate of Long Freezing Range Alloys," *AFS Cast Met. Res. J.*, 1972, *8*, pp. 1-6.
10. D.R. Durham and J.T. Berry: "Role of the Mold-Metal Interface During Solidification of a Pure Metal Against a Chill," *AFS Trans.*, 1976, *84*, pp. 101-29.
11. K. Ho and R.D. Pehlke: "Transients Methods for Determination of Metal Mold Interfacial Heat Transfer," *AFS Trans.*, 1983, *91*, pp. 689-98.
12. A.A. Ashish: "Development and Implementation of a Computer Code for Inverse Modelling of Heat Transfer with Application to Materials Processing," M.Tech. Dissertation, Mangalore University, Karnataka Regional Engineering College, Srinivasnagar 574157, India, 2001.
13. J.V. Beck: "Non Linear Estimation Applied to the Non Linear Heat Conduction Problem," *J. Heat Transfer*, 1970, *13*, pp. 703-16.
14. J.V. Beck: "Transient Sensitivity Coefficients for the Thermal Contact Conductance," *Int. J. Heat Mass Transfer*, 1967, *10*, pp. 1615-17.